

Dynamic Models of Planar Sliding

Jiayin Xie¹ and Nilanjan Chakraborty²

¹ Stony Brook University, Stony Brook NY 11733, USA,
jiayin.xie@stonybrook.edu,

² Stony Brook University, Stony Brook NY 11733, USA,
nilanjan.chakraborty@stonybrook.edu

Abstract. In this paper, we present a principled method to model general planar sliding motion with distributed convex contact patch. The effect of contact patch with indeterminate pressure distribution can be equivalently modeled as the contact wrench at one point contact. We call this point *equivalent contact point*. Our dynamic model embeds ECP within the equations of slider's motion and friction model which approximates the distributed contact patch, and eventually brings us a system of quadratic equations. This discrete-time dynamic model allows us to solve for the two components of tangential friction impulses, the friction moment and the slip speed. The state of the slider as well as the ECP can be computed by solving a system of linear equations once the contact impulses are computed. In addition, we derive the closed form solutions for the state of slider for quasi-static motion. Furthermore, in pure translation case, based on the discrete-time model, we present the closed form expressions for the friction impulses the slider suffers and the state of it at each time step. Simulation examples are shown to demonstrate the validity of our approach.

1 Introduction

In robotic manipulation, a key problem is how to move an object from one configuration to another. There are two ways of manipulating objects, namely, prehensile manipulation and non-prehensile manipulation. In prehensile manipulation, the robot grasps the object and moves it so that all the external wrenches acting on the object through manipulator or gripper during the motion is resisted. In non-prehensile manipulation one manipulates an object without grasping the object. Examples of non-prehensile manipulation includes throwing [1,2,3], batting [4,5], pushing [6,7,8,9] and vibratory motion [10,11]. For non-prehensile manipulation, where the object being manipulated slides over a support surface, a key aspect to designing planning and control algorithms is the ability to predict the motion of the sliding object. In this paper, our goal is to study the problem of motion prediction of an object sliding on a support surface.

A key aspect of planar sliding motion is that there is usually a non-point patch contact between the slider (or sliding object) and the support. The state of the slider depends on the applied external forces and the friction forces which distribute over the contact patch. The effect of the contact patch can be modeled

equivalently by the sum of the total distributed normal and tangential force acting at one point and the net moment about this point due to the tangential contact forces. This point is called the *center of friction* in [9]. If we assume that the motion of the slider is quasi-static (i.e., the inertial forces are negligible and thus the friction forces balance the applied forces), the center-of-friction lies directly below the center of mass, and closed-form expressions can be developed for motion prediction [6,8,9]. However, for dynamic sliding, when the inertial forces cannot be neglected, the center of friction can move around in the contact patch, and there is no method in the literature for computing it.

The existing approach is to use a dynamic simulation algorithm with contact patch usually approximated with three support points (chosen in ad-hoc manner). The reason for choosing three support points is that most dynamic simulation algorithms that are usually used for motion prediction implicitly assumes a point contact model and choosing 3 support points ensure that the force distribution at the three points is unique (if four or more points are used, the force distribution will not be unique for the same equivalent force and moment acting on the object). If the center of friction lies within the convex hull of the chosen support points, the motion predicted will be accurate. However, if the center of friction is outside the convex hull, then the predicted motion will not be accurate. Furthermore, since we do not know the center of friction, we will not know when the predicted motion is inaccurate. Note that the accuracy issue arises here due to the ad hoc approximation of the patch contact and not due to other sources of inaccuracy like contact friction model or model parameters.

In this paper, based on our previous work of nonlinear complementarity problem-based dynamic time-stepper with convex contact patch [12], we present a dynamic model for sliding, where no ad hoc approximation is made for the patch contact. We model the patch contact with a point contact, called the *equivalent contact point* (ECP). *The ECP is defined as a unique point in the contact patch where the net moment due to the normal contact force is zero [12].* We show that the computation of the contact forces/impulses and the state of the object and ECP can be decoupled for planar sliding. The contact impulses can be computed by solving four quadratic equations in four variables, namely, the two components of tangential impulse, the frictional moment, and the slip speed. The state variables, namely, the position, orientation, linear and angular velocities of the object as well as the ECP can be computed by solving a system of linear equations once the contact impulses are computed. *Note that the ECP as defined here is the same as the center of friction.* The presentation of the decoupled set of quadratic and linear equations for computing the contact impulse, the ECP, and the state of the slider is the key contribution of this paper. We show that closed form solutions for the state of the slider can be derived for quasi-static motion (which is same as those previously obtained in the literature). For pure translation also, closed form solutions can be derived for the contact impulse, the state of the object and the ECP. We also present numerical simulation results comparing the model that we derive to the solution of the NCP model from [12].

2 Related work

During the sliding motion, the friction plays an important role in determining the motion of object. Our model assumes Coulomb's friction law (also called Amonton, da vinci or dry friction law) [13]. Coulomb suggests that the friction force should be proportional to the normal force and opposed to the direction of sliding. The constant of proportionality is called coefficient of friction.

There has been many efforts to extend Coulomb's law into general sliding planar motion (Jellett [14], Prescott [15], MacMillan [16] and Mason [9]). As we have mentioned, the pressure distribution of the contact patch is usually unknown. Rather than assuming uniform pressure distribution as a coarse approximation for the unknown distribution, MacMillan assumes a linear pressure distribution. And he observes that [16]: during a pure translation, the system of frictional forces arising in the contact area may be reduced to a single force acting through a fixed point: *center of friction*. He uses center of friction to determine the friction force and moment during the translation.

Mason [9] generalizes MacMillan's center of friction to arbitrary pressure distributions. The definition of center of friction is:

$$\mathbf{x}_o = \frac{1}{\lambda_n} \int_R \mathbf{x} p(\mathbf{x}) dA \quad (1)$$

where \mathbf{x}_o is the center of friction, λ_n is the total support force, R represents the region of contact patch, dA is the differential element of area of R , \mathbf{x} is position of dA and $p(\mathbf{x})$ is the pressure distribution at \mathbf{x} . Mason use center of friction for determining whether an object will rotate when it is pushed and its rotation direction: *voting theorem*.

Furthermore, Mason claims that center of friction is computable based on the knowledge of external forces and moments, i.e.,:

$$\mathbf{x}_o = -\frac{1}{\lambda_n} \begin{bmatrix} \tau_y \\ \tau_x \end{bmatrix} \quad (2)$$

where τ_x and τ_y represent the total applied moments on horizontal axes (x and y axes). This is true due to the fact that:

All the applied forces and moments should balance each other to guarantee planar surface contact between slider and support plane, which fixes the position of center of friction.

Other than the usage in voting theorem, or in pure translation motion, center of friction can be useful in general sliding motion. Based on Equation (1), center of friction is also the point where the net moment due to the normal contact force is zero, i.e., $\int_R (\mathbf{x} - \mathbf{x}_o) p(\mathbf{x}) dA = 0$. Therefore, the effect of contact patch can be modeled equivalently by the net wrench acting at this point due to the distributed contact forces. And thus, we give center of friction a new name: *equivalent contact point* (ECP). Once we can compute ECP along with its contact wrench during the motion, the motion of the slider can be determined without the knowledge of pressure distribution.

Unfortunately, Equation (2) usually is not useful for computing ECP: without providing the exact knowledge of external forces and moments (including applied and friction forces), the ECP is not computable. Furthermore, the acceleration of a body whose positions of external forces (contact point of pushing, center of gravity, etc.) are above or below the support plane will, in general, cause the shift in the pressure distribution and corresponding shift in the center of friction or ECP [17].

Because of the computing difficulty and shift issue of ECP, previous pushing models [6,8] are addressed based on quasi-static assumption. In addition, they implicitly assume that the center of mass or gravity and contact point of pushing should lie on the horizontal support plane. Therefore, with uniform coefficient of friction assumption, the center of friction or ECP will just beneath or coincide with the center of mass [16].

Rather than solving the ECP and friction forces separately, our dynamic model embeds ECP within the friction model. Therefore, the ECP together with its contact wrench are computable. There has been much attempt to model and understand the effect of non-point frictional contact [18,19,20]. In this paper, we use a generalized friction model which considers the moment due to frictional distributed forces. The model is called soft-finger contact model [21].

3 Mechanics of planar sliding

3.1 Problem formulation

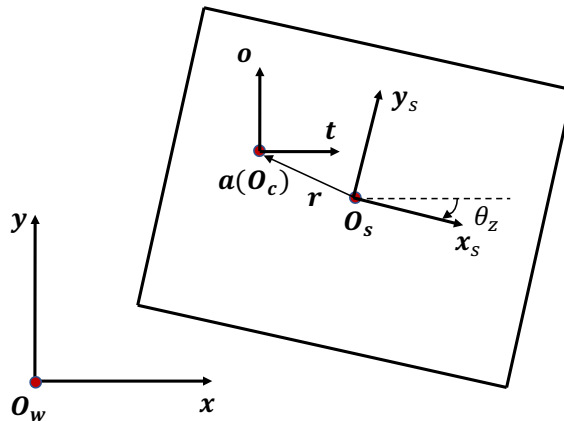


Fig. 1: Slider with square contact patch on the horizontal support plane.

In Figure 1, the slider is a rigid body and has horizontal patch contact with the support surface $\mathcal{W} = \mathcal{R}^2$. A world frame $\mathcal{F}_w \in \mathcal{R}^2$ with origin O_w is fixed on the support surface. The slider frame $\mathcal{F}_s \in \mathcal{R}^2$ with origin O_s is attached to the

slider's center of mass. The orientation of \mathcal{F}_s relative to \mathcal{F}_w is θ_z . In addition, there exists contact frame $\mathcal{F}_c \in \mathcal{R}^2$ with origin \mathbf{O}_c . The origin \mathbf{O}_c coincides with \mathbf{a} , the equivalent contact point (ECP). Furthermore, the axes of \mathcal{F}_c is parallel to \mathcal{F}_w . In this paper, we assume the contact patch as a convex patch. We also assume that the slider moves in the horizontal support surface without toppling, and it is allowed to rotate about the normal axis. Therefore, the configuration and state space of the slider is $\mathcal{R}^2 \times \mathcal{S}^1$. Here we define the configuration of the slider as $\mathbf{q} = [q_x, q_y, \theta_z]$, where q_x and q_y is the horizontal position of CM. State of the slider is $\boldsymbol{\nu} = [v_x, v_y, w_z]$, where v_x and v_y is the tangential components of CM's velocity and w_z is the angular velocity about normal axis.

The external forces acting on the slider includes applied force, gravity force, normal or support force and frictional force. We assume the applied force to be horizontal and the moment it produces is about the normal axis. Therefore, the generalized applied force can be $\boldsymbol{\lambda}_{app} = [\lambda_x, \lambda_y, \lambda_z\tau]$. The position of gravity force is CM (q_x, q_y, q_z) , where q_z is CM's vertical distance above support plane. Therefore, in general, the position of gravity force should be above the support plane. The related shift issue of ECP would be discussed in Section 3.2.

Now, let's consider the frictional force. We assume that the frictional force between slider and support surface conforms to Coulomb's law. At any contact, the tangential frictional force λ_f should satisfy the relationship: $\lambda_f \leq \mu\lambda_n$, where μ is the coefficient of friction and λ_n is the normal force at contact. In this paper, we always assumes a uniform coefficient of friction. In planar sliding motion, the normal force is distributed over the contact patch, which is called the pressure distribution. In general, the pressure distribution is indeterminate. In addition, to consider moments due to the distributed friction force, we generalize the Coulomb's law to include frictional moments in the direction of normal axis. The contact wrench between slider and support plane is defined with contact frame \mathcal{F}_c . Let λ_n be the sum of distributed normal force of the contact patch. The tangential components of friction force and moment are $(\lambda_t, \lambda_o, \lambda_r)$.

In next section, we define the problem of general planar sliding motion with distributed pressure distribution mathematically.

3.2 Equations of planar sliding motion

The motion of the slider is based on Newton-Euler equations. Let's first consider the general 3D motion of a rigid body. For a rigid body in \mathcal{R}^3 space, its motion can be described as:

$$\mathbf{M}(\mathbf{q})\dot{\boldsymbol{\nu}} = \mathbf{W}_n\lambda_n + \mathbf{W}_t\lambda_t + \mathbf{W}_o\lambda_o + \mathbf{W}_r\lambda_r + \boldsymbol{\lambda}_{app} + \boldsymbol{\lambda}_{vp} \quad (3)$$

where $\mathbf{M}(\mathbf{q}) \in \mathcal{R}^{6 \times 6}$ is the inertia tensor, $\mathbf{q} \in \mathcal{R}^6$ describes both position and orientation of the rigid body. $\boldsymbol{\nu} \in \mathcal{R}^6$ is the state of the object which contains both linear and angular velocity components in \mathcal{R}^3 space. $\boldsymbol{\lambda}_{app} \in \mathcal{R}^6$ is the vector of the external forces and moments. $\boldsymbol{\lambda}_{vp}$ represents the centripetal and Coriolis forces. Let \mathbf{W}_n , \mathbf{W}_t , \mathbf{W}_o and \mathbf{W}_r be the unit wrench which maps the

contact forces and moment λ_n , λ_t , λ_o and λ_r to the world frame. The expressions of unit wrenches are:

$$\begin{aligned} \mathbf{W}_n &= \begin{bmatrix} \mathbf{n} \\ \mathbf{r} \times \mathbf{n} \end{bmatrix} & \mathbf{W}_t &= \begin{bmatrix} \mathbf{t} \\ \mathbf{r} \times \mathbf{t} \end{bmatrix} \\ \mathbf{W}_o &= \begin{bmatrix} \mathbf{o} \\ \mathbf{r} \times \mathbf{o} \end{bmatrix} & \mathbf{W}_r &= \begin{bmatrix} \mathbf{0} \\ \mathbf{n} \end{bmatrix} \end{aligned} \quad (4)$$

where $(\mathbf{n}, \mathbf{t}, \mathbf{o}) \in \mathcal{R}^3$ is the axis of contact frame \mathcal{F}_c in \mathcal{R}^3 space. $\mathbf{0} \in \mathcal{R}^3$ is a vector with each entry equal to zero. The $\mathbf{r} \in \mathcal{R}^3$ is the vector from ECP to CM.

In the case of general planar sliding motion, as mentioned in Section 3.1, the configuration of the slider is $\mathbf{q} = [q_x, q_y, \theta_z]$ and the state vector is $\boldsymbol{\nu} = [v_x, v_y, w_z]$. Therefore, the inertial tensor becomes $\mathbf{M} = \text{diag}(m, m, I_z)$, where m is the mass of the slider and I_z represents the moment of inertia about normal axis. The external forces are $\boldsymbol{\lambda}_{app} = [\lambda_x, \lambda_y, \lambda_{z\tau}]$. After simplifying Equations (3) and (4), we get the formulation for planar sliding motion:

$$m\dot{v}_x = \lambda_t + \lambda_x \quad (5)$$

$$m\dot{v}_y = \lambda_o + \lambda_y \quad (6)$$

$$I_z\dot{w}_z = \lambda_r + \lambda_{z\tau} \quad (7)$$

Equations (5), (6) and (7) are the equations of planar sliding motion, which also describes how the state of the slider (v_x, v_y, w) is affected by the friction forces $(\lambda_t, \lambda_o, \lambda_r)$. In addition, the support normal force balances with the gravity force:

$$\lambda_n - mg = 0 \quad (8)$$

Derived from Equations (3) and (4), we can also obtain the following constraints:

$$I_x\dot{w}_x = p_{x\tau} + p_n(a_y - q_y) - p_o(a_z - q_z) + I_y w_y w_z - I_z w_y w_z \quad (9)$$

$$I_y\dot{w}_y = p_{y\tau} - p_n(a_x - q_x) + p_t(a_z - q_z) - I_x w_x w_z + I_z w_x w_z \quad (10)$$

where I_x and I_y are the moment of inertia about tangential axes. w_x and w_y , \dot{w}_x and \dot{w}_y are the angular velocity and acceleration about tangential axes, in planar sliding case without toppling, they should equal to zero. $\lambda_{x\tau}$ and $\lambda_{y\tau}$ represents the applied moments about tangential axes. As we have already assumed previously, the applied forces can only produce the moment about the normal axis, i.e., $\lambda_{z\tau}$. Therefore $\lambda_{x\tau} = \lambda_{y\tau} = 0$. Eventually, we can get the expressions for ECP:

$$a_x = -\lambda_t q_z / \lambda_n + q_x \quad (11)$$

$$a_y = -\lambda_o q_z / \lambda_n + q_y \quad (12)$$

Equations (11) and (12) provide us a closed form expressions for ECP based on the given friction forces. When $q_z = 0$, ECP (a_x, a_y) would just beneath the CM (q_x, q_y) . When $q_z > 0$, i.e., CM is above the support plane, ECP shifts from CM.

Furthermore, the variance of tangential friction forces (λ_t and λ_o) would cause the shift of ECP during the motion. This is called the shift issue of ECP.

In this subsection, we derive the equations of motion for general planar sliding. In addition, we get the closed form expression of ECP. However, to eventually compute the state of the object and ECP, we need to know the value of friction forces. In next subsection, we will introduce a generalized Coulomb friction model to approximate the distributed contact patch between slider and support plane.

3.3 Ellipsoid friction model

We use a friction model based on the maximum power dissipation principle and generalizes Coulomb's friction law, i.e., among all the possible contact forces and moments that lie within the friction ellipsoid, the forces that maximize the power dissipation of the contact patch are selected.

$$\begin{aligned} \max \quad & -(v_t \lambda_t + v_o \lambda_o + v_r \lambda_r) \\ \text{s.t.} \quad & \left(\frac{\lambda_t}{e_t}\right)^2 + \left(\frac{\lambda_o}{e_o}\right)^2 + \left(\frac{\lambda_r}{e_r}\right)^2 - \mu^2 \lambda_n^2 \leq 0 \end{aligned} \quad (13)$$

We use the contact wrench at ECP to model the effect of entire distributed contact patch. Therefore v_t and v_o are the tangential components of velocity at ECP. v_r is the relative angular velocity about the normal at ECP. Let e_t, e_o and e_r be the given positive constants defining the friction ellipsoid and let μ represents the coefficient of friction at the contact [20,22]. This constraint is the elliptic dry friction condition suggested in [20] based upon evidence from a series of contact experiments. In planar sliding case, the tangential velocity at ECP are $[v_t, v_o]^T = \mathbf{v} + \mathbf{w} \times \mathbf{r}$. Thus:

$$v_t = v_x - w_z(a_y - q_y) \quad (14)$$

$$v_o = v_y + w_z(a_x - q_x) \quad (15)$$

$$v_r = w_z \quad (16)$$

Equation (13) has a useful alternative formula [23]:

$$0 = e_t^2 \mu \lambda_n v_t + \lambda_t \sigma \quad (17)$$

$$0 = e_o^2 \mu \lambda_n v_o + \lambda_o \sigma \quad (18)$$

$$0 = e_r^2 \mu \lambda_n v_r + \lambda_r \sigma \quad (19)$$

$$0 \leq \mu^2 \lambda_n^2 - \lambda_t^2/e_t^2 - \lambda_o^2/e_o^2 - \lambda_r^2/e_r^2 \perp \sigma \geq 0 \quad (20)$$

where σ represents the magnitude of sliding velocity at ECP.

In planar sliding case, the slider keeps sliding on the surface, thus, $\sigma > 0$ during the motion. Therefore, the complementarity Equation (20) can be simplified as:

$$\mu^2 \lambda_n^2 - \lambda_t^2/e_t^2 - \lambda_o^2/e_o^2 - \lambda_r^2/e_r^2 = 0 \quad (21)$$

In next section, we combine the equations of planar sliding motion with the friction model to derive the dynamic model of planar sliding.

4 Planar sliding motion dynamic model

4.1 Continuous-time dynamic model

Equations (14), (15) and (16) together with the friction model (Equations (17), (18), (19), (21)) describe our continuous-time planar sliding dynamic model.

$$0 = \mu\lambda_n e_t^2 [v_x - w_z(a_y - q_y)] + \lambda_t \sigma \quad (22)$$

$$0 = \mu\lambda_n e_o^2 [v_y + w_z(a_x - q_x)] + \lambda_o \sigma \quad (23)$$

$$0 = \mu\lambda_n e_r^2 w_z + \lambda_r \sigma \quad (24)$$

$$0 = \mu^2 \lambda_n^2 - \lambda_r^2 / e_r^2 - \lambda_t^2 / e_t^2 - \lambda_o^2 / e_o^2 \quad (25)$$

In Section 5.1, we utilize this continuous-time dynamic model for deriving the equation of quasi-static sliding motion.

4.2 Discrete-time dynamic model

We use backward Euler time-stepping scheme to discretize equations of planar sliding motion (Equations (5), (6) and (7)). Let t_u denote the current time and h be the duration of the time step, the superscript u represents the beginning of the current time and the superscript $u + 1$ represents the end of the current time. Let $\dot{\boldsymbol{\nu}} \approx (\boldsymbol{\nu}^{u+1} - \boldsymbol{\nu}^u)/h$, the impulse $p_{(\cdot)} = h\lambda_{(\cdot)}$:

$$m(v_x^{u+1} - v_x^u) = p_t^{u+1} + p_x^u \quad (26)$$

$$m(v_y^{u+1} - v_y^u) = p_o^{u+1} + p_y^u \quad (27)$$

$$I_z(w_z^{u+1} - w_z^u) = p_r^{u+1} + p_{z\tau}^u \quad (28)$$

Based on Equations (26), (27) and (28), we can rewrite our continuous-time dynamic formula into time-stepping scheme:

$$0 = \mu p_n e_t^2 \left\{ v_x^u + \frac{p_t^{u+1} + p_x^u}{m} + \frac{p_o^{u+1} q_z [w_z^u + (p_r^{u+1} + p_{z\tau}^u)/I_z]}{p_n} \right\} + p_t^{u+1} \sigma^{u+1} \quad (29)$$

$$0 = \mu p_n e_o^2 \left\{ v_y^u + \frac{p_o^{u+1} + p_y^u}{m} - \frac{p_t^{u+1} q_z [w_z^u + (p_r^{u+1} + p_{z\tau}^u)/I_z]}{p_n} \right\} + p_o^{u+1} \sigma^{u+1} \quad (30)$$

$$0 = \mu p_n e_r^2 [w_z^u + (p_r^{u+1} + p_{z\tau}^u)/I_z] + p_r^{u+1} \sigma^{u+1} \quad (31)$$

$$0 = \mu^2 p_n^2 - (p_r^{u+1}/e_r)^2 - (p_t^{u+1}/e_t)^2 - (p_o^{u+1}/e_o)^2 \quad (32)$$

Eventually, our dynamic model becomes system of quadratic equations, which contains four equations and four unknown variables (the friction impulses p_t, p_o, p_r and sliding velocity σ).

In next section, based on our continuous-time model, we prove that our model can be viewed as generalization of the model based on quasi-static assumption. In addition, based on our discrete-time model, we present analytical formula for pure translation based on our model. In Section 6, we use our quadratic discrete-time model for numerical computation.

5 Closed Form Equations For Planar Sliding Motion

5.1 Quasi-static sliding motion

The quasi-static sliding motion [8] studies a pusher-slider system with point contact. According to quasi-static assumption, the pusher pushes the slider at low velocities. In this situation, frictional forces dominate the motion of the slider, and inertial force can be neglected. Based on the equations of sliding motion (Equations (5), (6) and (7)), the friction force and applied force should balance with each other (i.e., $\lambda_t = -\lambda_x$, $\lambda_o = -\lambda_y$, $\lambda_r = -\lambda_z\tau$). We assume that the pusher sticks with the slider during the motion. Therefore, the motion of the slider depends on the motion of the pusher:

$$v_x = v_{px} + w_z(y_c - q_y) \quad (33)$$

$$v_y = v_{py} - w_z(x_c - q_x) \quad (34)$$

where v_{px} and v_{py} represent the velocity of pusher, x_c and y_c represent the position of contact point between pusher and slider.

In addition, the applied force passes through the contact point, and it should balance with the friction force. Therefore, the friction moment about normal axis balances with the applied moment and it can be defined by the friction force:

$$\lambda_r = (x_c - q_x)\lambda_o - (y_c - q_y)\lambda_t \quad (35)$$

Quasi-static model also assumes that the ECP or center of friction is just beneath the CM. Thus, $a_x = q_x$, $a_y = q_y$. In addition, the model assumes isotropic friction. Therefore, the given constants of friction ellipsoid $e_t = e_o$. Let's define the parameter $c = e_r/e_t$. From Equation (22), (23), and (24), we get:

$$\frac{v_x}{w_z} = c^2 \frac{\lambda_t}{\lambda_r} \quad (36)$$

$$\frac{v_y}{w_z} = c^2 \frac{\lambda_o}{\lambda_r} \quad (37)$$

Eventually, we use equations above for solving the state of the slider (v_x, v_y, w_z):

$$v_x = \frac{[c^2 + (x_c - q_x)^2]v_{px} + (x_c - q_x)(y_c - q_y)v_{py}}{c^2 + (x_c - q_x)^2 + (y_c - q_y)^2} \quad (38)$$

$$v_y = \frac{[c^2 + (y_c - q_y)^2]v_{py} + (x_c - q_x)(y_c - q_y)v_{px}}{c^2 + (x_c - q_x)^2 + (y_c - q_y)^2} \quad (39)$$

$$w_z = \frac{(x_c - q_x)v_y - (y_c - q_y)v_x}{c^2} \quad (40)$$

If we locate the origin at the CM, $q_x = q_y = 0$. Thus, the equations of motion above would be equivalent to the equations of Quasi-static motion [8] of sticking contact case.

5.2 Pure translation

In this section, we derive the closed form expression for pure translation motion. During a pure translation motion, all the points in the slider move in the same direction. Thus, the slider's angular velocity remain zero, i.e., $w_z = 0$. In this case, we derive the closed form formula for the friction impulses that slider suffers during the motion. Furthermore, we derive the equations of pure translation motion.

The deviation is based on our discrete-time dynamic model (Equations (29), (30), (31) and (32)). Because $w_z = 0$ for each time step, based on Equation (31), the friction angular impulse $p_r = 0$. Therefore, Equations (29), (30) and (32) can be simplified as:

$$p_t^{u+1} = \frac{-e_t^2 \mu p_n (mv_x^u + p_x^u)}{m\sigma^{u+1} + e_t^2 \mu p_n} \quad (41)$$

$$p_o^{u+1} = \frac{-e_o^2 \mu p_n (mv_y^u + p_y^u)}{m\sigma^{u+1} + e_o^2 \mu p_n} \quad (42)$$

$$\mu^2 p_n^2 = (p_t^{u+1}/e_t)^2 + (p_o^{u+1}/e_o)^2 \quad (43)$$

Then substituting Equations (41) and (42) into (43), we get:

$$\frac{(mv_x^u + p_x^u)^2}{(m\sigma^{u+1} + e_t^2 \mu p_n)^2} + \frac{(mv_y^u + p_y^u)^2}{(m\sigma^{u+1} + e_o^2 \mu p_n)^2} = 1 \quad (44)$$

Given the isotropic friction assumption, i.e., $e_t = e_o$, we get:

$$m\sigma^{u+1} + e_t^2 \mu p_n = \sqrt{(mv_x^u + p_x^u)^2 + (mv_y^u + p_y^u)^2} \quad (45)$$

Thus, the analytical solutions for friction impulse are:

$$p_t^{u+1} = \frac{-e_t^2 \mu p_n (mv_x^u + p_x^u)}{\sqrt{(mv_x^u + p_x^u)^2 + (mv_y^u + p_y^u)^2}} \quad (46)$$

$$p_o^{u+1} = \frac{-e_o^2 \mu p_n (mv_y^u + p_y^u)}{\sqrt{(mv_x^u + p_x^u)^2 + (mv_y^u + p_y^u)^2}} \quad (47)$$

Therefore, we get the equations of motion:

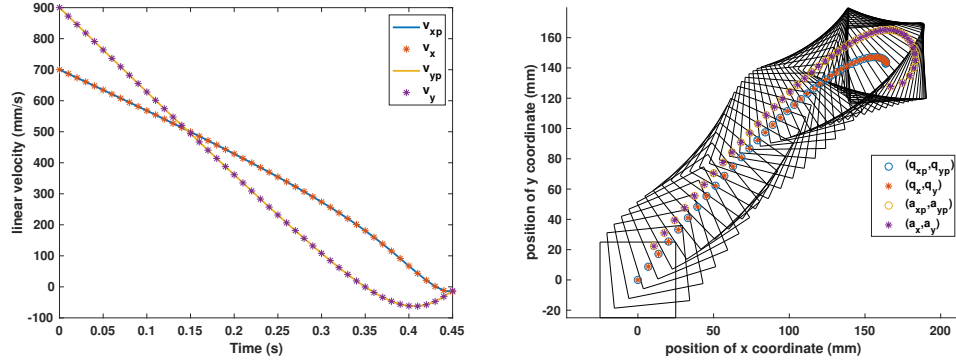
$$v_x^{u+1} = (p_t^{u+1} + p_x^u)/m + v_x^u \quad (48)$$

$$v_y^{u+1} = (p_o^{u+1} + p_y^u)/m + v_y^u \quad (49)$$

where p_t^{u+1} and p_o^{u+1} are given by Equations (46) and (47).

In this section, we derive the closed form expressions of motion for both quasi-static motion and pure translation motion with isotropic friction assumption. In general, there does not exist analytical solutions for the general planar sliding motion. Therefore, in next section, we present numerical solution for general planar sliding motion based on our discrete-time model.

6 Numerical Results

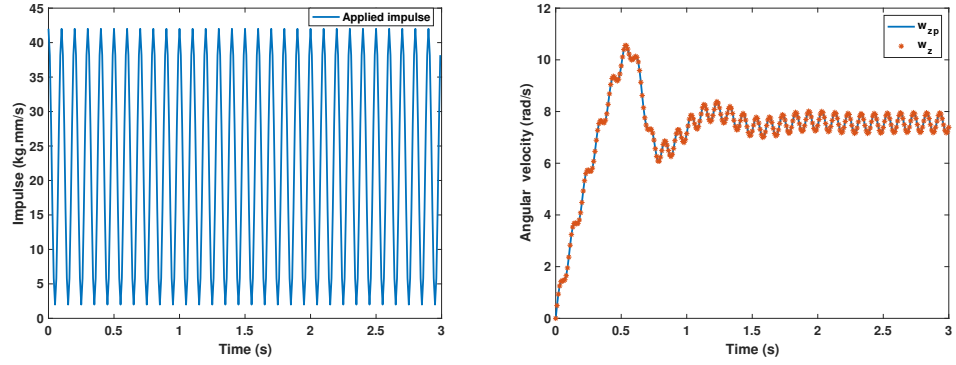


(a) The tangential components of slider's translational velocity. The result based on our simulation result. Furthermore, the position of quadratic model (v_x and v_y) overlaps with the CM and ECP based on discrete-time model solution from our NLP-based model (v_{xp} and v_{yp}). (b) The snapshot of slider's motion based on simulation result. Furthermore, the position of quadratic model (q_x, q_y and a_x, a_y) coincide with the result based on geometric scheme (q_{xp}, q_{yp} and a_{xp}, a_{yp}).

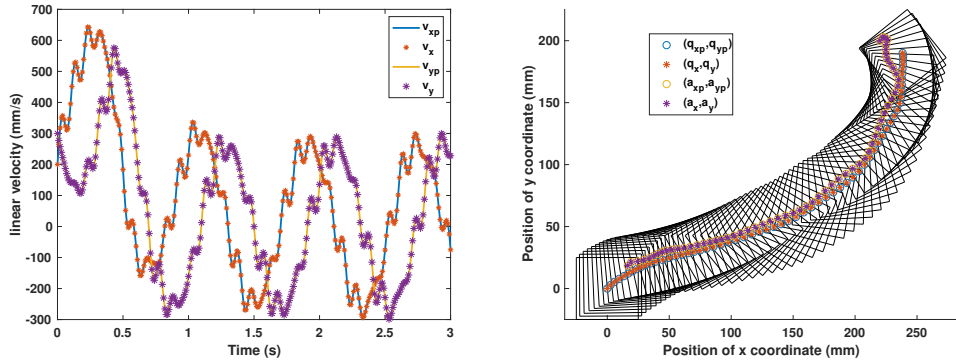
Fig. 2: The slider with square contact patch slides on the surface without external forces. During the motion, instead of overlapping the CM, the ECP separates from CM and varies within the contact patch.

The first example is for a slider with square contact patch sliding on the horizontal surface. The problem can be modeled with our discrete-time dynamic model (quadratic model). In addition, the problem can also be modeled based on our geometric time-stepping scheme [12] (NCP-based model), in which we utilize the geometrical information of the objects to formulate the contact constraints that prevents the penetration. Besides, the complementarity relationships for each contact mode (sliding, sticking, or separating) are also taken into account. We compare solutions from two schemes to validate our technique against our previous NCP-based approach, which gives the correct solution. In the second example, we provide a scenario of the slider being pushed with external force. The external force acts on one side of the slider and its position is fixed. The magnitude of external force is periodic and is always perpendicular to the slider. We use this example to show that the slider with external force can be modeled with our scheme.

We use 'fsolve' in MATLAB, which is based on 'trust-region-dogleg' algorithm, to solve the quadratic model. We use PATH complementarity solver [24] to solve NCP-based models. We compare the average time taken per time-step based on different models for the first example. All the examples are imple-



(a) Magnitude of periodical applied impulse. (b) The angular velocity w_z about normal axis.



(c) The tangential components of slider's translational velocity. (d) The snapshot of slider's motion from $t = 0$ s to $t = 0.6$ s.

Fig. 3: Slider with square contact patch being pushed by applied force.

mented in Matlab and run times are obtained on a Macbook Pro with 2.6 GHZ processor and 16 GB RAM.

6.1 Slider on a plane

In this example, we let a slider with square contact patch slide on the surface. The time step chosen for our discrete-time formula and geometric time-stepping scheme is $h = 0.01s$ and simulation time is $0.45s$. The coefficient of friction between slider and support plane is $\mu = 0.31$, and the friction ellipsoid's given positive constants are: $e_t = e_o = 1$, $e_r = 0.01m$. The mass of the slider is $m = 0.5kg$, and the gravity's acceleration is $g = 9.8m/s^2$. The slider slides on the surface without external force. It's initial position of CM is $q_x = q_y = 0m$, $q_z = 0.08m$. Initial orientation is $\theta = 0^\circ$. The initial state of slider is $v_x = 0.7m/s$, $v_y = 0.9m/s$ and $w_z = 10rad/s$.

As Figure 2 illustrates, a slider slides on the horizontal supporting surface. The forces that the slider suffers are friction forces and moments. In Figure 2a, we compute the state of the slider (v_x and v_y) numerically based on our discrete-time dynamic model (Equations (29), (30), (31), (32)), and compare it with the result (v_{xp} and v_{yp}) from NCP-based model. Eventually, there exists no difference between two results (within numerical tolerance of $1e-6$ and it converges), which validates our method. In addition, the average time that NCP-based model spends for each time-step is $0.0081s$, our quadratic model's average time is $0.0049s$. This is because our model essentially is a system of 4 quadratic equations with 4 variables (there are also a few linear equations afterwards, but the computational cost of those are negligible), and thus the size and complexity of the system are much less than the NCP-based model (in sliding case, the system is composed of 24 nonlinear equations and unknowns).

In Figure 2b, we plot the snapshots of the slider's contact patch with CM and ECP at each time step. The contact patch's shape is the square with length $L = 0.05m$ and width $W = 0.05m$. During the motion, we observe that the position of ECP always separates from the position of CM, and it varies its relative position to the slider frame \mathcal{F}_s within the contact patch. The observation conforms the shift issue of ECP: when the position of center of mass is above the support plane, acceleration of object would cause the shift of ECP [17].

6.2 Slider being pushed on a plane

In the second example, we let the slider be pushed by applied force on the horizontal plane. The dimension and mass of the slider as well as the friction parameters (μ , e_t , e_o and e_r) keep the same as previous example. In this example, we change the initial state of slider to be $v_x = 0.2m/s$, $v_y = 0.3m/s$ and $w_z = 0rad/s$. The time-step is still $0.01s$ and simulation time is extended to $3s$. During the motion, as shown in Figure 3d, we apply the force on the left edge of the square patch. The position of external force on the edge is fixed at $2.5mm$ below the middle of the edge. Let applied force always be perpendicular to that side

during the motion. As Figure 3a illustrates, the magnitude of the applied force is periodic, i.e.,

$$F_{push} = 2.2 + 2 \cos(2\pi t/T) \text{ N}$$

where the period $T = 0.1s$.

From Figure 3b, we compute the angular velocity about normal axis w_z based on our quadratic model and w_{zp} based on our NCP-based model. For Figure 3c, we compute the tangential components of velocity v_x, v_y based on our quadratic model, and v_{xp}, v_{yp} based on our NCP-based model. For both angular and tangential velocities, the difference between quadratic and NCP solutions is within the numerical tolerance of $1e-6$. Figure 3d plot the snapshot of the slider at each time step between the time period from $t = 0s$ to $t = 0.6s$.

7 Conclusions

In this paper, we present a quadratic discrete-time dynamic model for solving the problem of general planar sliding with distributed convex contact patch. Previous method assumes quasi-static motion or chooses multiple contact points (usually three) in an ad-hoc manner to approximate the entire contact patch. In our dynamic model, the effect of contact patch is equivalently modeled as the contact wrench at the *equivalent contact point*. During the motion, the balance of all the external forces and moments including gravity force, applied force and frictional force fixes the position of ECP. Therefore, by combing the equation of motion with friction model, we get the quadratic discrete-time model. This allows us to solve two components of tangential friction impulses, the friction moment and the slip speed. The state of the slider as well as the ECP can be computed by solving a system of linear equations once the contact impulses are computed. In addition, we also provide closed form expression for quasi-static motion and pure translation motion. We also demonstrate the numerical results based on our quadratic model and NCP model for the general planar motion of the slider with or without applied force.

References

1. M. T. Mason and K. M. Lynch, "Dynamic manipulation," in *Intelligent Robots and Systems' 93, IROS'93. Proceedings of the 1993 IEEE/RSJ International Conference on*, vol. 1. IEEE, 1993, pp. 152–159.
2. W. H. Huang, E. P. Krotkov, and M. T. Mason, "Impulsive manipulation," in *Robotics and Automation, 1995. Proceedings., 1995 IEEE International Conference on*, vol. 1. IEEE, 1995, pp. 120–125.
3. C. Zhu, Y. Aiyama, T. Chawanya, and T. Arai, "Releasing manipulation," in *Intelligent Robots and Systems' 96, IROS 96, Proceedings of the 1996 IEEE/RSJ International Conference on*, vol. 2. IEEE, 1996, pp. 911–916.
4. R. L. Andersson, *A Robot Ping-pong Player: Experiment in Real-time*. MIT Press, 1988.

5. C. Liu, Y. Hayakawa, and A. Nakashima, "Racket control and its experiments for robot playing table tennis," in *Robotics and Biomimetics (ROBIO), 2012 IEEE International Conference on*. IEEE, 2012, pp. 241–246.
6. K. M. Lynch and M. T. Mason, "Stable pushing: Mechanics, controllability, and planning," *The International Journal of Robotics Research*, vol. 15, no. 6, pp. 533–556, 1996.
7. K. M. Lynch, "Locally controllable manipulation by stable pushing," *IEEE Transactions on Robotics and Automation*, vol. 15, no. 2, pp. 318–327, 1999.
8. K. M. Lynch, H. Maekawa, and K. Tanie, "Manipulation and active sensing by pushing using tactile feedback," in *IROS*, 1992, pp. 416–421.
9. M. T. Mason, "Mechanics and planning of manipulator pushing operations," *The International Journal of Robotics Research*, vol. 5, no. 3, pp. 53–71, 1986.
10. T. H. Vose, P. Umbanhowar, and K. M. Lynch, "Vibration-induced frictional force fields on a rigid plate," in *Robotics and Automation, 2007 IEEE International Conference on*. IEEE, 2007, pp. 660–667.
11. —, "Friction-induced lines of attraction and repulsion for parts sliding on an oscillated plate," *IEEE Transactions on Automation Science and Engineering*, vol. 6, no. 4, pp. 685–699, 2009.
12. J. Xie and N. Chakraborty, "Rigid body dynamic simulation with line and surface contact," in *Simulation, Modeling, and Programming for Autonomous Robots (SIMPAN), IEEE International Conference on*. IEEE, 2016, pp. 9–15.
13. C. A. Coulomb, *Théorie des machines simples en ayant égard au frottement de leurs parties et à la roideur des cordages*. Bachelier, 1821.
14. J. H. Jellett, *A Treatise on the Theory of Friction*. Hodges, Foster, 1872.
15. J. Prescott and D. S. MA, *Mechanics of particles and rigid bodies*. Longmans, Green, 1929.
16. W. D. MacMillan, "Dynamics of rigid body," 1936.
17. M. T. Mason, *Mechanics of robotic manipulation*. MIT press, 2001.
18. M. Erdmann, "On a representation of friction in configuration space," *The International Journal of Robotics Research*, vol. 13, no. 3, pp. 240–271, 1994.
19. S. Goyal, A. Ruina, and J. Papadopoulos, "Planar sliding with dry friction part 1. limit surface and moment function," *Wear (Amsterdam, Netherlands)*, vol. 143, no. 2, pp. 307–330, 1991.
20. R. D. Howe and M. R. Cutkosky, "Practical force-motion models for sliding manipulation," *The International Journal of Robotics Research*, vol. 15, no. 6, pp. 557–572, 1996.
21. R. M. Murray, *A mathematical introduction to robotic manipulation*. CRC press, 2017.
22. J. C. Trinkle, J.-S. Pang, S. Sudarsky, and G. Lo, "On dynamic multi-rigid-body contact problems with coulomb friction," *ZAMM-Journal of Applied Mathematics and Mechanics/Zeitschrift für Angewandte Mathematik und Mechanik*, vol. 77, no. 4, pp. 267–279, 1997.
23. J. C. Trinkle, J. Tzitzouris, and J.-S. Pang, "Dynamic multi-rigid-body systems with concurrent distributed contacts," *Philosophical Transactions of the Royal Society of London A: Mathematical, Physical and Engineering Sciences*, vol. 359, no. 1789, pp. 2575–2593, 2001.
24. S. P. Dirkse and M. C. Ferris, "The path solver: A non-monotone stabilization scheme for mixed complementarity problems," *Optimization Methods and Software*, vol. 5, no. 2, pp. 123–156, 1995.